Published in final edited form as:
Nat Cell Biol. 2016 June ; 18(6): 684–691. doi:10.1038/ncb3344.

Centromeric DNA replication reconstitution reveals DNA loops and *ATR* checkpoint suppression

Antoine Aze[1,2], **Vincenzo Sannino**[1], **Paolo Soffientini**[1], **Angela Bachi**[1], and **Vincenzo Costanzo**[1,*]

[1]DNA Metabolism Laboratory, IFOM, The FIRC Institute of Molecular Oncology, Via Adamello 16, Milan, 20139, Italy

Abstract

Half of human genome is made of repetitive DNA. However, mechanisms underlying replication of chromosome regions containing repetitive DNA are poorly understood. We reconstituted replication of defined human chromosome segments using Bacterial Artificial Chromosomes (BACs) in *Xenopus laevis* egg extract. Using this approach we characterized chromatin assembly and replication dynamics of centromeric alpha-satellite DNA. Proteomic analysis of centromeric chromatin revealed replication dependent enrichment of a network of DNA repair factors among which the *MSH2-6* complex, which was required for efficient centromeric DNA replication. However, contrary to expectations, the *ATR* dependent checkpoint monitoring DNA replication fork arrest could not be activated on highly repetitive DNA due to inability of single stranded DNA binding protein *RPA* to accumulate on chromatin. Electron microscopy of centromeric DNA and supercoil mapping revealed the presence of Topoisomerase I dependent DNA loops embedded in a protein matrix enriched for *SMC2-4* proteins. This arrangement suppressed *ATR* signalling by preventing *RPA* hyper-loading, facilitating replication of centromeric DNA. These findings have important implications on our understanding of repetitive DNA metabolism and centromere organization under normal and stressful conditions.

Repetitive sequences can impair DNA replication adopting unusual conformations and predisposing to genome instability1–3. Centromeric DNA in many species contains 171-bp repeat arrays, known as alpha-satellite DNA4, which contribute to centromere structure formation5, 6. To understand repetitive DNA replication dynamics we studied replication of defined human chromosome segments in *Xenopus laevis* egg extract using BACs. We showed that large circular BACs formed functional nuclei, which were able to import cytoplasmic Green Fluorescent Protein containing a nuclear localization signal (GFP-NLS) (Fig. 1a-b). Such BACs were fully replicated by semiconservative DNA synthesis, and

*Corresponding author: Vincenzo.costanzo@ifom.eu.
[2]Current address: Replication and Genome Dynamics Laboratory, Institute of Human Genetics, CNRS, Rue de la Cardonille 141, Montpellier, 34396, France

Author contributions

A.A. and V.S. prepared the materials and performed the experiments. P.S. and A.B. performed mass spectrometry analysis. A.A. and V.C. designed, analysed and wrote the manuscript.

Europe PMC Funders Author Manuscripts

replication together with replication initiation complex assembly was sensitive to geminin, the *MCM2-7* loading inhibitor7, and roscovitin, a Cyclin Dependent Kinase (*CDK*) inhibitor8, although their replication time was slower than the time commonly required for sperm replication (Fig. 1c-f and Supplementary Fig. 1a-f). For these studies we used BACs containing human centromeric alpha-satellite DNA or repeat-free DNA regions with similar GC base content (Supplementary Fig. 1g-j). For most of the experiments shown we compared non-centromeric RP11-1151L10 (or L10) and centromeric RP11-5B18 (or B18) BACs. Replication efficiencies of L10, B18 and other different BACs, and chromatin binding of replication proteins on L10 and B18 were overall similar (Fig. 1f and Supplementary Fig. 1k-n). However, centromeric B18 replication kinetic was slower than non-centromeric L10 at early time points (Fig. 1g). This was likely due to the repetitive nature of the centromeric DNA impacting on replication fork progression. Replicated L10 and B18 isolated at 3.5 hours from replication initiation instead did not show detectable differences in the initiation rate and had an average inter origin distance (IOD) of 16 kb, similar to sperm nuclei (Fig. 1h-i and Supplementary Fig. 1o). Interestingly, centromeric DNA selectively recruited *CENP-A*, the histone H3 variant specifically enriched on centromeric chromatin9 (Fig. 1j).

To identify proteins enriched on centromeric DNA or depleted from it during DNA synthesis we set up quantitative mass spectrometry (MS) of L10 and B18 chromatin isolated from extract using LC–MS-MS analysis and label-free protein quantification (See Methods and Supplementary Fig. 2a). Several proteins resulted differentially associated with L10 and B18 BACs (Fig. 2a-c, Table S1, S2 and S3). Geminin dependent inhibition of many B18 bound proteins suggested their involvement in centromeric DNA replication (Fig. 2b and 2c). Many B18 enriched and geminin sensitive factors had a known function in DNA repair such as the mismatch repair (MMR) proteins *MSH2-6*, the *MRE11-RAD50* complex, *HMGB1-3*, *XRCC1*, *XRCC5* and *PARP1,* and formed a network with other enriched repair factors (Fig. 2a, 2c and Supplementary Fig 2b). Also enriched on centromeric DNA were chromosome structural components *SMC2-4*, common subunits of Condensin I and II complexes10 and henceforth collectively referred to as Condensins (Fig. 2a). Other DNA metabolism proteins such as members of the *RPA* complex and *TopBP1* were instead under-represented on centromeric DNA (Fig. 2a). Other B18 bound proteins belonged to pathways not previously associated to repetitive DNA. MS results for several proteins were validated by western blot (WB) as shown in Supplementary Fig. 2c-e and throughout the manuscript.

Repair factors enrichment and slower replication kinetics suggested the presence of abnormal structures in centromeric DNA impacting on replication fork progression. To verify this hypothesis we analyzed the *ATR* dependent checkpoint, which can be activated by replication stress11, by monitoring *CHK1* Serine 345 phosphorylation (*pCHK1*) in L10 and B18 nuclei. Surprisingly, fork stalling induced by DNA polymerase inhibitor aphidicholin12 did not induce *CHK1* phosphorylation in B18 nuclei (Fig. 3a-b). *RPA* protein complex accumulation on ssDNA is critical to activate *ATR*11. We noticed decreased *RPA* binding and a significant reduction in its accumulation induced by aphidicolin onto B18 DNA compared to L10 (Fig. 3c-d). Chromatin levels of *TopBP1,* which requires *RPA* to load onto DNA13, were also lower on centromeric DNA, although decreased levels of *RPA* were still able to promote normal *ATR* binding (Supplementary Fig. 2c-d). Intriguingly,

aphidicolin treatment stimulated further centromeric DNA loading of *MSH2-6* proteins (Fig. 3e lanes 2-4 and Fig. 3f), whose levels on B18 chromatin were already higher than L10 (Fig. 3e lanes 1-3, Fig. 3f and Supplementary Fig. S2c and 2e). Significantly, B18 replication in extracts depleted of *MSH6*14 was impaired, indicating that *MSH6* is required for efficient centromeric DNA replication (Fig. 3g-h).

To understand centromeric DNA organization we performed Electron Microscopy (EM) using a protocol previously established15 (See also Methods). In addition to the expected replication intermediates we noticed large regions of single stranded DNA (ssDNA bubbles) up to 1000 ± 200 bp in size, distributed along centromeric DNA (Fig. 4a) and absent on non-centromeric DNA (Supplementary Fig. 3a) or naked B18 templates (Supplementary Fig. 3b). ssDNA bubbles were not replication intermediates, which are made of double stranded DNA (dsDNA) (Supplementary Fig. 3c) and not of ssDNA (Supplementary Fig. 3d). ssDNA bubbles were abolished by geminin (Supplementary Fig. 3e), were more frequent than replication intermediates (Fig. 4a), were rarely associated to centromeric replication forks (Supplementary Fig. 3f) and were unlikely to be the product of degraded DNA replication intermediates as overall efficiency of B18 and L10 replication was similar. We hypothesized that ssDNA bubbles arose from DNA regions resistant to psoralen crosslinking, which was used to stabilize endogenous DNA structures for the EM procedure (Supplementary Fig. 4a). Positively supercoiled DNA, which is enriched on centromeric chromatin16, 17 is highly refractory to psoralen crosslinking18, 19 and might give rise to ssDNA bubbles after melting in the mild denaturing conditions used for to spread DNA for EM (Supplementary Fig. 4b). To verify the presence of positively supercoiled DNA regions we performed DNA supercoil mapping, a procedure based on the ability of biotynilated psoralen (bPsoralen) to incorporate preferentially in negatively underwound DNA and poorly in positively overwound DNA18, 19. Following bPsoralen photocrosslinking of intact L10 and B18 nuclei bPsoralen incorporation was monitored by dot blot using streptavidin-HRP (Fig. 4b) or a fluorescence energy transfer (FRET) based assay (Fig. 4c). These experiments revealed low levels of bPsoralen incorporation in centromeric B18 DNA, suggesting the presence of overwound DNA.

We then investigated the mechanisms responsible for this topological arrangement. Condensins promote positive supercoiling of DNA *in vitro* in the presence of Topoisomerase I10. Centromeric chromatin accumulation of Condensins revealed by MS and confirmed by WB (Supplementary Fig. 5a-b) prompted us to test whether overwound DNA was actively formed in the presence of Condensins and Topoisomerase I. To this end we used Topoisomerase I inhibitor topotecan (TPT)20. TPT prevented accumulation of positively supecoiled DNA on centromeric DNA (Fig. 4b-c). bPsoralen incorporation in TPT treated DNA was not due to DNA breakage (Supplementary Fig. 5c). Also, TPT did not affect centromeric DNA bound Condensins (Supplementary Fig. 5d). These observations suggested that Topoisomerase I, possibly together with Condensins, was involved in the formation of overwound DNA regions on centromeric DNA.

Since positive supercoiling limits DNA unwiding21 we asked whether this topological arrangement was responsible for *RPA* chromatin binding inhibition. Remarkably, TPT restored normal *RPA* loading and accumulation on centromeric chromatin (Fig. 4d-e).

To verify whether intereference with centromeric DNA topology had an effect on the activation of the *ATR* dependent checkpoint we monitored *ATR* activity using a more sensitive assay previoulsy established22, which is based on histone H2AX phosphorylation. This assay confirmed that *ATR* was not activated by stalled forks arising on centromeric DNA (Fig. 4f), showing also lower basal levels of checkpoint singalling on untreated centromeric DNA. Consistent with the effects on *RPA* chromatin binding, TPT treatment was able to restore normal *ATR* dependent checkpoint activation on centromeric DNA in the presence of aphidicolin (Fig. 4f).

To understand the physiological significance of *ATR* checkpoint suppression we tested the effect of restoring *ATR* signalling using TPT and aphidicolin at concentrations that did not inhibit the bulk of DNA polymerization but which were able to induce limiting amount of ssDNA23 and *ATR* activity (Fig. 4f). Significantly, centromeric DNA replication was inhibited by low levels of *ATR* activity and could be restored by an *ATR* specific inhibitor (Fig. 4g). Taken together these data suggested that suppression of *ATR* signalling facilitates centromeric DNA replication.

During early stages of mitosis Condensins and Topoisomerases initiate a process that leads to chromosome condensation, in which DNA is organized in large DNA loops held together by a protein matrix10. Condensins play important but poorly understood roles in the general organization of chromosomes and centromeres10. Overwound DNA regions in the centromere might underlie the presence of DNA loops linked to Condensins. To uncover the presence of these structures and to visualize them we isolated chromatin under limiting protein digestion conditions that preserved sufficient amounts of DNA bound proteins able to maintain centromeric chromatin structure (Supplementary Fig. 5e-f and Methods). Using this approach we observed dsDNA loops that were distributed at either sides of centromeric DNA (Fig. 5a). We could not distinctively visualize the matrix holding the loops probably due to EM shadowing interference caused by the DNA, although granules and other structures with different electrondensity were observed (Fig. 5a). To verify that DNA loops were held by a protein matrix milder extraction conditions were followed by complete proteinase K mediated digestion (Supplementary Fig. S5e-f and Methods). This led to DNA loop disappearance and revealed the presence of ssDNA bubbles similar to the ones described earlier (Fig. 5b). We counted about 20-25 loops every 50 kB of DNA with an average size for each loop from base to apex of 1000 ± 200 bp. DNA loops were absent in geminin treated samples (Fig. 5c), suggesting that they were actively formed and stabilized by proteins loaded on centromeric DNA during or after DNA replication initiation. Loops were stably mantained over time (Fig. 5c) and inhibition of Topoisomerase I prevented loop formation, although it did not perturb loops already formed (Fig. 5d), suggesting that superhelical tension, which could be easily lost during DNA isolation, was involved in DNA loop formation but not maintainance.

Here we successfully reconstituted replication of defined chromosome regions in *Xenopus laevis* egg extract. We established the proteome of a specific human chromosome segment during its replication, revealing the structure, the replication dynamics and the replication stress response of centromeric DNA. We showed that efficient centromeric DNA replication requires MMR proteins, which can bind mismatched hairpins and other DNA secondary

structures24, 25, and are probably involved in their resolution, facilitating replication fork progression (Fig. 5e, panel a). Such structures can form on alpha-satellite DNA repetitive units, which harbor conserved palindromic regions of homopurine and homopyrimidine elements that can pair following DNA unwinding26, 27, potentially altering fork progression. In the presence of replication stress caused by aphidicolin extensive ssDNA regions generated by helicase uncoupling28 might generate even more hairpins29 causing further MMR proteins accumulation on centromeric DNA (Fig. 5e, panel b).

Using EM we directly observed the ultrastructural organization of centromeric DNA, uncovering the presence of dsDNA loops, which might be held by a Condensin enriched protein matrix. Condensins could promote formation of DNA loops by an extrusion-based (loop extrusion)30, 31 or by Topoisomerase-dependent mechanism (chiral loops)10. Positively supercoiled DNA and Condensin complex II enrichment have previuosly been observed at centromeres10, 16. DNA loops dependency on replication and Topoisomerase I suggest that they are actively formed as replication progresses. Topoisomerase II participation in this process cannot be ruled out. Inefficient centromere replication in the absence of *MSH2-6* might also affect their formation.

The presence of dsDNA loops might reflect centromeric DNA organization in the interphase nucleus during early chromosome condensation processes10, which might start from the centromere in interphase and spread to other regions of the chromosomes in mitosis. DNA loop formation might be facilitated by Topoisomerase-induced superhelical tension in the context of centromeric nucleosome fibers and might require both chiral and extrusion-based mechanisms. Interestingly, Condensins promote *CENP-A* chromatin binding9. However, *CENP-A* loading kinetic on centromeric BAC is different from somatic cells, in which *CENP-A* chromatin recruitment takes place between telophase and early G132, and might not entirely reflect new *CENP-A* molecules loading onto pre-existing centromeres. Selective accumulation mechanisms of *CENP-A* and Condensins onto centromeric BAC, respective roles of Condensin I and II complexes in loop formation and their involvement in *CENP-A* loading remain to be clarified.

Accumulation of DNA loops must be coordinated with DNA replication to allow replication fork progression21 and it is likely to take place behind forks (Fig. 5e, panel a). The observed dsDNA loops resemble previously proposed centromeric loops organized in spring-like structures linked centromere and kinetochore function in mitosis17. However, we uncovered another function for this structural organization showing that this arrangement prevents the exposure of extended regions of ssDNA and consequent *RPA* hyper-loading in conditions of replication stress (Fig. 5e, panel b). Physically constrained DNA loops in the nucleus accumulating behind forks could limit the extent of normal fork movements and rotation33, restraining helicase mediated DNA unwinding needed for *RPA* chromatin binding11 (Fig. 5e, panel b). As *RPA* hyper-loading is required to promote chromating binding of *ATR* activating cofactors, among which *TopBP1*11, 13, restraining *RPA* binding to chromatin prevents full activation of the *ATR* dependent checkpoint, which normally limits DNA replication origin firing under stress11 (Fig. 5e, panel b). Interference with centromeric DNA topology restores normal *RPA* loading and promotes activation of *ATR*, which inhibits DNA replication (Fig. 5e, panel c). Suppression of *ATR* activity facilitates replication of

repetitive centromeric DNA, whose natural tendency to form DNA secondary structures can slow down replication fork progression. Therefore, the *ATR* dependent checkpoint triggered by secondary DNA structures arising in the context of repetitive DNA could be locally suppressed by DNA loops that form as replication progresses, facilitating completion of DNA replication.

Checkpoint suppression is common to other chromosome regions containing repetitive DNA such as telomeres34, which can form DNA loops and can be organized in positively supercoiled domains by telomeric proteins35. The experimental approach described here will be useful to dissect the role of checkpoint, DNA repair and structural proteins at repetitive chromosome loci, whose aberrant metabolism can predispose to cancer and other human diseases.

Supplementary Material

Refer to Web version on PubMed Central for supplementary material.

Acknowledgements

We thank H. Mahbubani and F. Pezzimenti for technical support with *Xenopus Laevis*, J. Gannon for antibody production, M. Lopes for helpful discussions, J. Jiricny for MMR antibodies and A. Losada for *CENP-A* antibodies. This work was funded by the Associazione Italiana per Ricerca sul Cancro (AIRC), the European Research Council (ERC) Consolidator grant (614541), the Giovanni Armenise-Harvard foundation award, the Epigen Progetto Bandiera (4.7), the AICR-Worldwide Cancer Research (13-0026) and the Fondazione Telethon (GGP13-071) grant awarded to V.C. A.B. is funded by AIRC grant IG 14578.

References

1. Mirkin SM. Expandable DNA repeats and human disease. Nature. 2007; 447:932–940. [PubMed: 17581576]
2. Zhao J, Bacolla A, Wang G, Vasquez KM. Non-B DNA structure-induced genetic instability and evolution. Cellular and molecular life sciences : CMLS. 2010; 67:43–62. [PubMed: 19727556]
3. Zeman MK, Cimprich KA. Causes and consequences of replication stress. Nature cell biology. 2014; 16:2–9. [PubMed: 24366029]
4. Murphy TD, Karpen GH. Centromeres take flight: alpha satellite and the quest for the human centromere. Cell. 1998; 93:317–320. [PubMed: 9590164]
5. Rudd MK, Wray GA, Willard HF. The evolutionary dynamics of alpha-satellite. Genome research. 2006; 16:88–96. [PubMed: 16344556]
6. Bloom KS. Centromeric heterochromatin: the primordial segregation machine. Annual review of genetics. 2014; 48:457–484.
7. McGarry TJ, Kirschner MW. Geminin, an inhibitor of DNA replication, is degraded during mitosis. Cell. 1998; 93:1043–1053. [PubMed: 9635433]
8. Meijer L, et al. Biochemical and cellular effects of roscovitine, a potent and selective inhibitor of the cyclin-dependent kinases cdc2, cdk2 and cdk5. European journal of biochemistry / FEBS. 1997; 243:527–536. [PubMed: 9030781]
9. Bernad R, et al. Xenopus HJURP and condensin II are required for CENP-A assembly. The Journal of cell biology. 2011; 192:569–582. [PubMed: 21321101]
10. Hirano T. Condensins: universal organizers of chromosomes with diverse functions. Genes & development. 2012; 26:1659–1678. [PubMed: 22855829]
11. Cimprich KA, Cortez D. *ATR*: an essential regulator of genome integrity. Nature reviews Molecular cell biology. 2008; 9:616–627. [PubMed: 18594563]

12. Errico A, Costanzo V. Mechanisms of replication fork protection: a safeguard for genome stability. Critical reviews in biochemistry and molecular biology. 2012; 47:222–235. [PubMed: 22324461]
13. Hashimoto Y, Tsujimura T, Sugino A, Takisawa H. The phosphorylated C-terminal domain of Xenopus Cut5 directly mediates *ATR*-dependent activation of CHK1. Genes to cells : devoted to molecular & cellular mechanisms. 2006; 11:993–1007. [PubMed: 16923121]
14. Olivera Harris M, et al. Mismatch repair-dependent metabolism of O-methylguanine-containing DNA in Xenopus laevis egg extracts. DNA repair. 2015; 28C:1–7. [PubMed: 25697728]
15. Hashimoto Y, Ray Chaudhuri A, Lopes M, Costanzo V. Rad51 protects nascent DNA from Mre11-dependent degradation and promotes continuous DNA synthesis. Nature structural & molecular biology. 2010; 17:1305–1311.
16. Furuyama T, Henikoff S. Centromeric nucleosomes induce positive DNA supercoils. Cell. 2009; 138:104–113. [PubMed: 19596238]
17. Bloom KS. Centromeric heterochromatin: the primordial segregation machine. Annual review of genetics. 2014; 48:457–484.
18. Bermudez I, Garcia-Martinez J, Perez-Ortin JE, Roca J. A method for genome-wide analysis of DNA helical tension by means of psoralen-DNA photobinding. Nucleic acids research. 2010; 38:e182. [PubMed: 20685815]
19. Naughton C, et al. Transcription forms and remodels supercoiling domains unfolding large-scale chromatin structures. Nature structural & molecular biology. 2013; 20:387–395.
20. Ray Chaudhuri A, et al. Topoisomerase I poisoning results in PARP-mediated replication fork reversal. Nature structural & molecular biology. 2012; 19:417–423.
21. Vos SM, Tretter EM, Schmidt BH, Berger JM. All tangled up: how cells direct, manage and exploit topoisomerase function. Nature reviews Molecular cell biology. 2011; 12:827–841. [PubMed: 22108601]
22. Costanzo V, Paull T, Gottesman M, Gautier J. Mre11 assembles linear DNA fragments into DNA damage signaling complexes. PLoS biology. 2004; 2:E110. [PubMed: 15138496]
23. Hashimoto Y, Puddu F, Costanzo V. RAD51- and MRE11-dependent reassembly of uncoupled CMG helicase complex at collapsed replication forks. Nature structural & molecular biology. 2012; 19:17–24.
24. Slean MM, Panigrahi GB, Ranum LP, Pearson CE. Mutagenic roles of DNA “repair” proteins in antibody diversity and disease-associated trinucleotide repeat instability. DNA repair. 2008; 7:1135–1154. [PubMed: 18485833]
25. Burdova K, Mihaljevic B, Sturzenegger A, Chappidi N, Janscak P. The Mismatch-Binding Factor MutSbeta Can Mediate *ATR* Activation in Response to DNA Double-Strand Breaks. Molecular cell. 2015; 59:603–614. [PubMed: 26212458]
26. Koch J. Neocentromeres and alpha satellite: a proposed structural code for functional human centromere DNA. Human molecular genetics. 2000; 9:149–154. [PubMed: 10607825]
27. Jonstrup AT, et al. Hairpin structures formed by alpha satellite DNA of human centromeres are cleaved by human topoisomerase IIalpha. Nucleic acids research. 2008; 36:6165–6174. [PubMed: 18824478]
28. Lupardus PJ, Byun T, Yee MC, Hekmat-Nejad M, Cimprich KA. A requirement for replication in activation of the *ATR*-dependent DNA damage checkpoint. Genes & development. 2002; 16:2327–2332. [PubMed: 12231621]
29. Voineagu I, Freudenreich CH, Mirkin SM. Checkpoint responses to unusual structures formed by DNA repeats. Molecular carcinogenesis. 2009; 48:309–318. [PubMed: 19306277]
30. Nasmyth K. Disseminating the genome: joining, resolving, and separating sister chromatids during mitosis and meiosis. Annual review of genetics. 2001; 35:673–745.
31. Sanborn AL, et al. Chromatin extrusion explains key features of loop and domain formation in wild-type and engineered genomes. Proceedings of the National Academy of Sciences of the United States of America. 2015
32. Dunleavy EM, et al. HJURP is a cell-cycle-dependent maintenance and deposition factor of CENP-A at centromeres. Cell. 2009; 137:485–497. [PubMed: 19410545]
33. Bermejo R, et al. The replication checkpoint protects fork stability by releasing transcribed genes from nuclear pores. Cell. 2011; 146:233–246. [PubMed: 21784245]

34. Palm W, de Lange T. How shelterin protects mammalian telomeres. Annual review of genetics. 2008; 42:301–334.

35. Amiard S, et al. A topological mechanism for TRF2-enhanced strand invasion. Nature structural & molecular biology. 2007; 14:147–154.

Europe PMC Funders Author Manuscripts

Europe PMC Funders Author Manuscripts

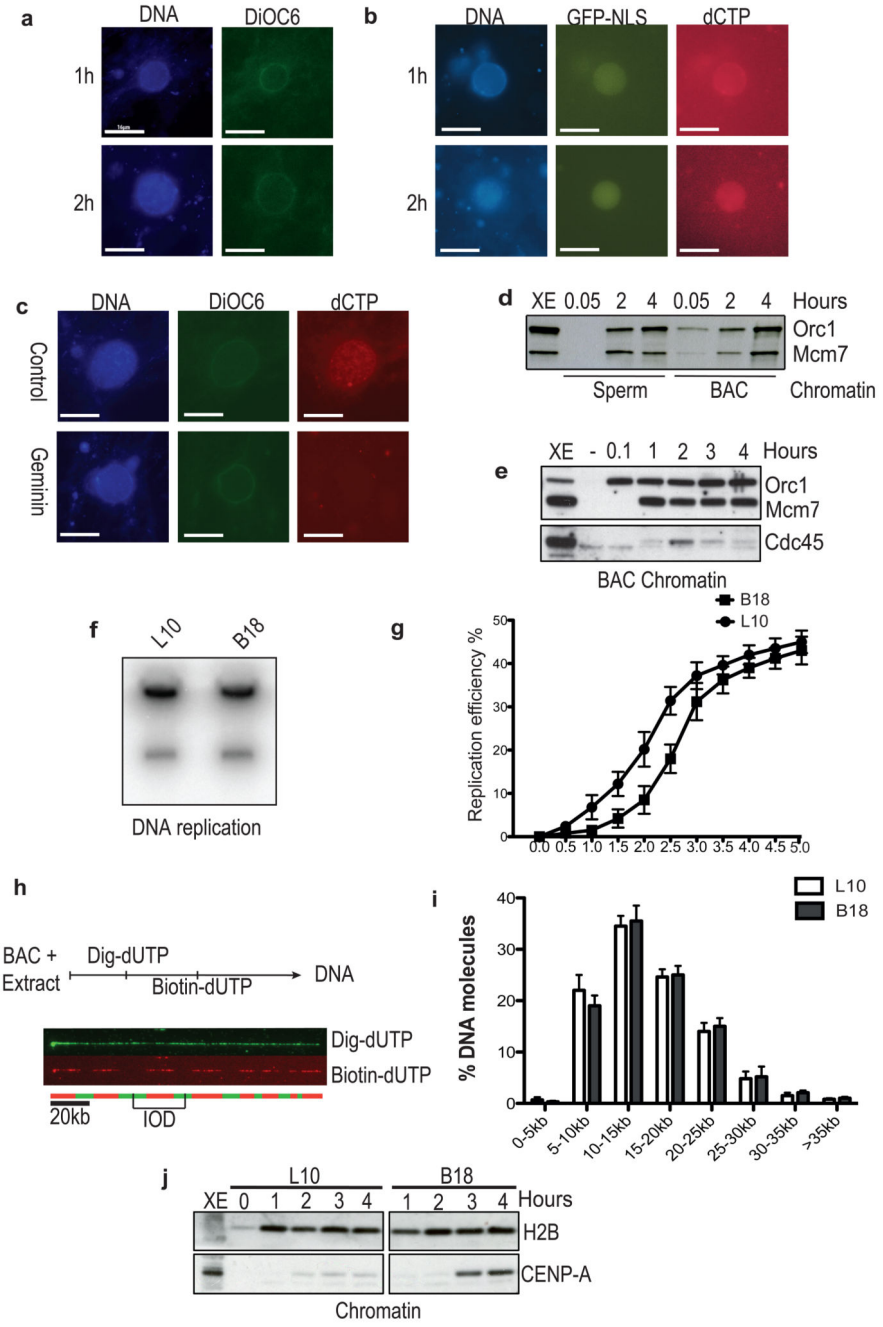

Figure 1. BAC DNA induced nuclei formation and DNA synthesis in interphase *Xenopus* egg extract.

(**a**) BACs were incubated in interphase extract for the indicated time. Samples were fixed and stained with DAPI for DNA (DNA) and DiOC6 for membranes (DiOC6). (**b**) Nuclei assembled in interphase extract supplemented with GFP-NLS and Cy3-dCTP (dCTP). (**c**) BACs replicated for 4 hours in egg extract supplemented with buffer (Control) or recombinant geminin (Geminin). (**d**) and (**e**) Chromatin isolated from sperm and BACs nuclei at different times and analysed by WB with the indicated antibodies. Representative

images of experiments performed at least three times are shown. (**f**) Autoradiography of non-centromeric (L10) and centromeric (B18) BACs replicated in the presence of ^{32}PdCTP. A representative image is shown. (**g**) Replication kinetics of non-centromeric L10 and centromeric B18 DNA. Error bars represent ± sd of the mean. *n=3 experiments; p<0.001 when comparing L10 and B18 mean values for all the indicated times; unpaired two-tailed t-test.* (**h**) Scheme of DNA combing experiment and example of DNA fiber visualization by immunofluorescence. BACs were incubated in egg extract, supplemented with Dig-dUTP (Green) and, at later time points, with Biotin-dUTP (Red). DNA was isolated at 3.5 hours from addition to egg extract for combing. Typical combing of L10 BAC is shown. Midpoints of green tracts (Dig-dUTP) represent origins of DNA replication (replication eye in the red track). Distance between midpoints of two adjacent replication eyes represents inter-origins distance (IOD) (**i**) Graph showing distribution percentage of IODs measured for control L10 (black) and B18 DNA (grey). At least hundred fibres were scored for each sample. Error bars represent ± sd of the mean. n=3 experiments; p<0.001 when comparing L10 and B18 mean values for all IODs; One-way Anova. (**j**) Chromatin was isolated at the indicated times of the replication reactions with L10 and B18 DNA and then analyzed by WB using the indicated antibodies. A representative of 3 experiments is shown. Uncropped gel images for all experiments are shown in Supplementary Figure 6.

Europe PMC Funders Author Manuscripts

Europe PMC Funders Author Manuscripts

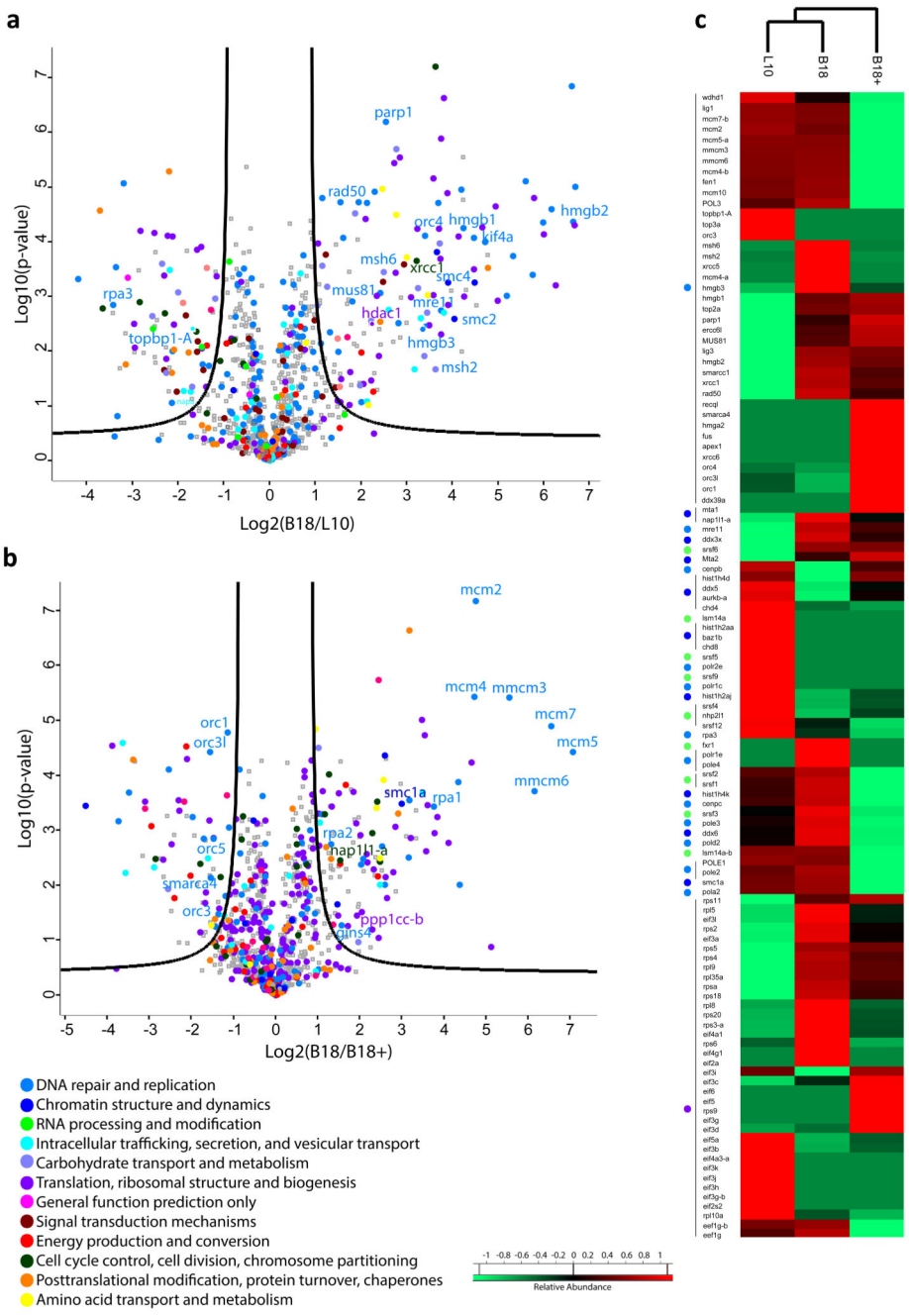

Figure 2. Proteomic analysis of replicating centromeric and non-cetromeric chromatin using label free quantitative MS.

(**a**) Centromeric B18 and non-centromeric L10 chromatin was isolated after 150 minutes incubation of BAC DNA in egg extract and analysed by high resolution MS-MS. Volcano plots show the mean $\log_2$ protein B18/L10 ratio plotted against the p-values of biological replicates. Proteins differentially represented on centromeric and non-centromeric chromatin are shown. Black lines indicate the significance cut off. (**b**) Proteins differentially represented on centromeric chromatin in the absence (B18) or in the presence (B18+) of

geminin analysed as in (a) are shown. Experiments shown in (a) and (b) were repeated with three different extracts (see Methods and Table S2 for statistical significance). (**c**) Heat map for some non-centromeric (L10) and centromeric (B18) or geminin sensitive (B18+) proteins. Chromatin enriched proteins are in red, depleted proteins in green.

Europe PMC Funders Author Manuscripts

Europe PMC Funders Author Manuscripts

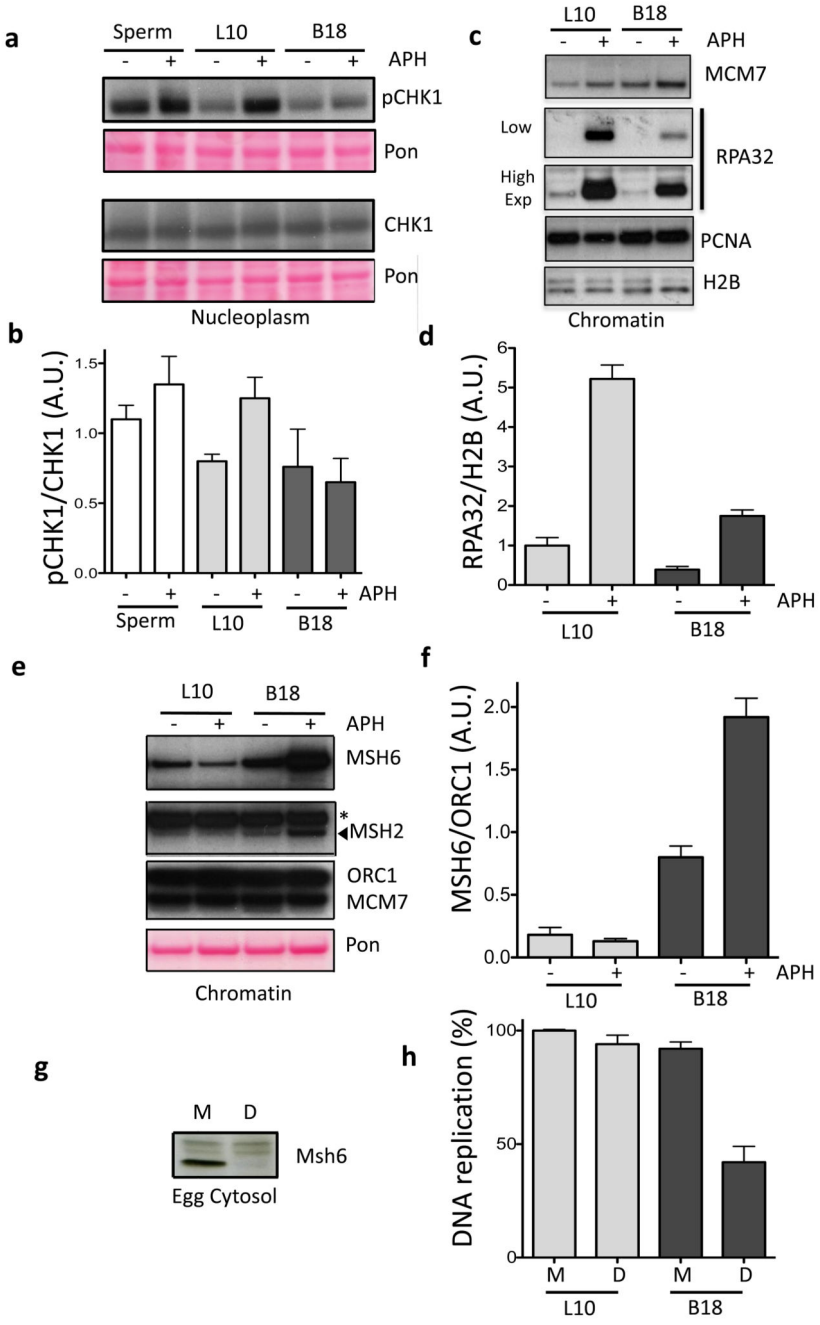

Figure 3. Centromeric DNA Replication is associated with checkpoint suppression and MMR proteins accumulation

(**a**) Sperm nuclei, L10 or B18 BACs were incubated in egg extract treated with 25 μg ml^{-1} aphidicolin (APH) (+) or buffer (-). Cytoplasmic *CHK1* and its phosphorylated form (*pCHK1*) were detected using specific antibodies as indicated. Total transferred proteins were stained with Ponceau (Pon). (**b**) The average ratio of *pCHK1* signal over the total level of *CHK1* was quantified and plotted in the graph. Error bars represent ± sd of the mean. *n*=5 independent experiments; $p<0.05$ when comparing Sperm, L10 and B18 mean values for

APH (+) or buffer (-) treated conditions; One-way Anova. (**c**) Chromatin from L10 and B18 BACs was isolated after 150 minutes of incubation in extracts supplemented with APH (+) or buffer (-). Samples were analysed by WB using antibodies against the indicated proteins. (**d**) Average ratio of *RPA*32 over Histone *H2B* (H2B) signal was quantified and shown in the graph. Error bars represent ± sd of the mean. n=7 independent experiments; $p<0.01$ when comparing L10 and B18 mean values for APH (+) or buffer (-) treated conditions; One-way Anova. (**e**) Chromatin from L10 and B18 BACs treated as in (c) was analysed by WB with the indicated antibodies. Total transferred proteins were stained with Ponceau (Pon). Asterisk indicates non-specific band. (**f**) Average ratio of MSH6 over ORC1 bound to chromatin was quantified and shown in the graph. Error bars represent ± sd of the mean. n=3 independent experiments; $p<0.05$ when comparing L10 and B18 mean values for APH (+) or buffer (-) treated conditions; One-way Anova. (**g**) WB of egg cytosol that was mock (M) or *MSH6* depleted (D) using anti *Xenopus MSH6* antibodies. A typical result is shown. (**h**) L10 and B18 DNA replication in mock (M) and *MSH6* depleted (D) extracts. Relative average percentage of ^{32}PdCTP incorporation is shown. L10 values in mock-depleted extracts were considered 100%. Error bars represent ± sd of the mean. n=3 experiments; $p<0.05$ when comparing L10 and B18 mean values for Mock (M) and MSH6 depleted extracts (D); One-way Anova.

Europe PMC Funders Author Manuscripts

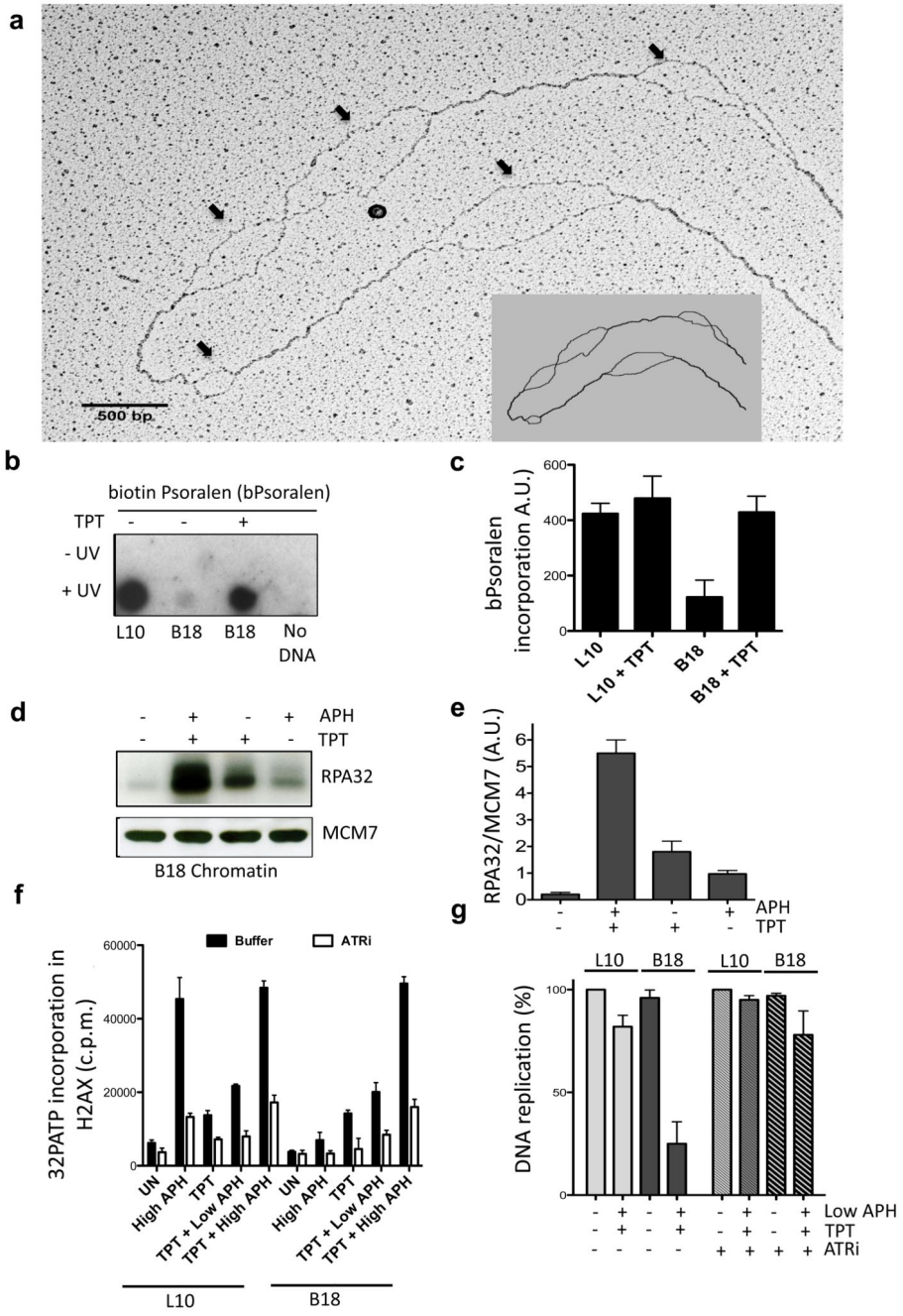

Figure 4. Overwound centromeric DNA suppresses *RPA* accumulation and *ATR* activation.

(**a**) EM of B18 DNA isolated after 150 minutes incubation in interphase extract. Arrows indicate ssDNA bubbles. Scheme is included. Data represent 1 out of 3 experiments. (**b**) Streptavidin-HRP stained dot blot of L10 ad B18 DNA isolated from BAC nuclei replicated with 40 μM topotecan (TPT) or left untreated and treated with biotin-psoralen (bPsoralen) in the presence (+) or absence (-) of UV. Data represent 1 out of 3 experiments (**c**) Total incorporated bPsoralen was measured using a fluorescence based biotin quantification assay. Values represent fluorescence intensity expressed in arbitrary units. Error bars represent ± sd

of the mean. n=3 experiments; p<0.05 when comparing L10 and B18 mean values for all treatments; One-way Anova. (**d**) WB of *RPA*32 and *MCM7* bound to B18 chromatin isolated from nuclei replicated in the presence of 40 μM topotecan (TPT) and 25 μg ml^{-1} APH as indicated. (**e**) *RPA*32/*MCM7* ratio. Error bars represent ± sd of the mean. n=3 experiments; p<0.01 when comparing B18 mean values for all treatments; One-way Anova. (**f**) Average incorporation of 32P in histone H2AX C-terminal peptide in the presence of nucleoplasm derived from L10 and B18 nuclei replicated in extracts that were untreated (UN), treated with 25 μg ml^{-1} APH (High APH), 40 μM TPT, TPT and 1 μg ml^{-1} APH (TPT + Low APH) or TPT and 25 μg ml^{-1} APH (TPT + High APH). Reactions were performed in the absence (black bars) or in the presence (white bars) of 10 μM VE-821 (*ATR*i). Error bars represent ± sd of the mean. n=3 experiments; p<0.001 when comparing B18 and L10 mean values for all treatments; One-way Anova. (**g**) L10 and B18 DNA replication in extracts treated with 40 μM TPT and 1 μg ml^{-1} APH (Low APH) in the presence or absence of ATRi as indicated. Relative average percentage of ^{32}PdCTP incorporation is shown. L10 values in untreated extracts were considered 100%. Error bars represent ± sd of the mean. n=3 experiments; p<0.001 when comparing B18 and L10 mean values for all treatments; One-way Anova.

Europe PMC Funders Author Manuscripts

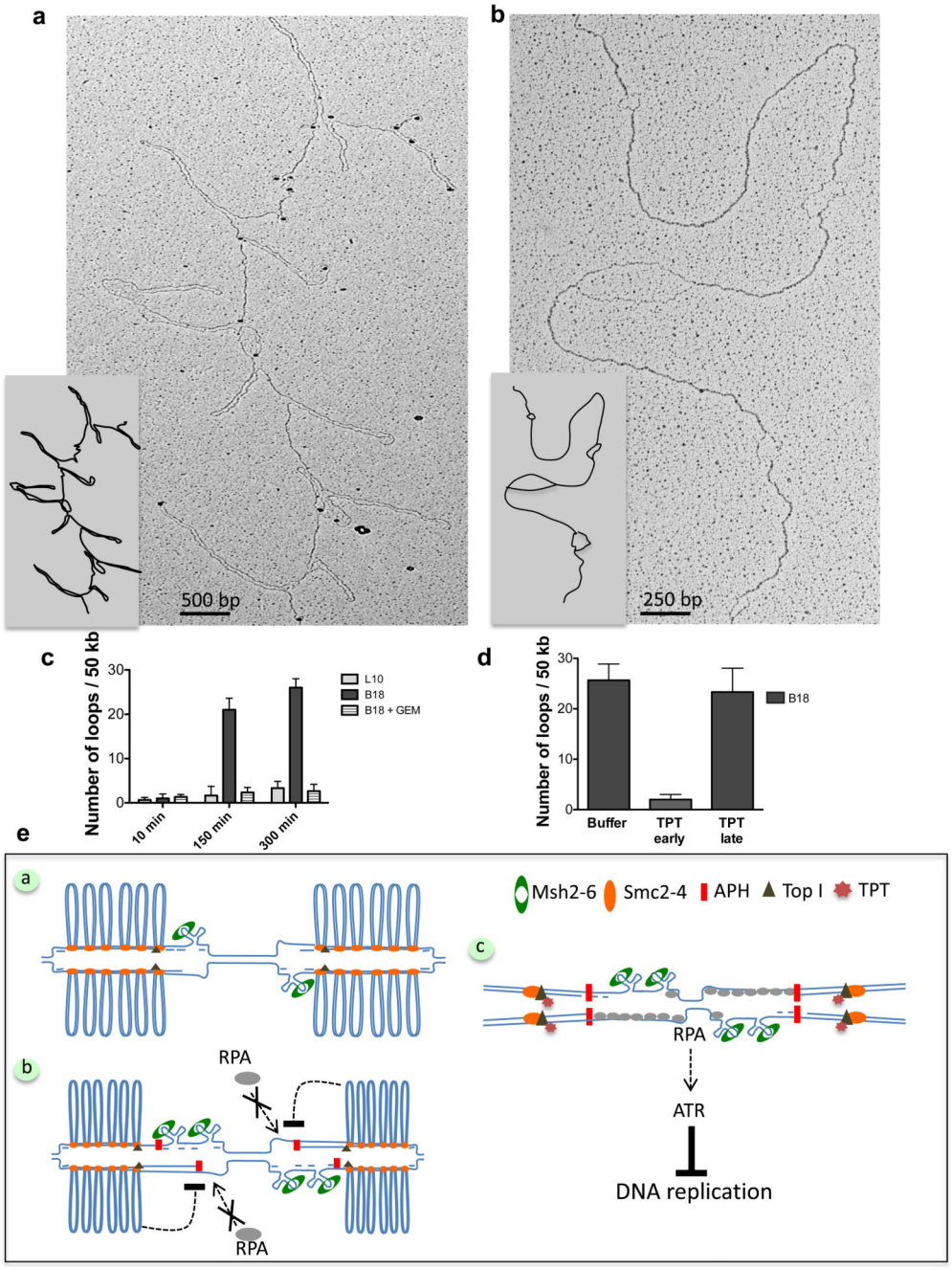

Figure 5. Centromeric BACs generate stable double stranded DNA loops during DNA replication.

(**a**) EM of centromeric B18 chromatin isolated after partial proteinase K digestion (See Methods). (**b**) EM analysis of samples isolated as in (**a**) and subjected to complete protein digestion. (**c**) Graph showing the frequency of DNA loops in L10 or B18 DNA incubated in extracts that were untreated or treated with geminin (Gem) for the indicated times. Experiments were repeated three times scoring the equivalent of about one mega base of DNA in total. Error bars represent ± sd of the mean. n=3 experiments; p<0.001 when

comparing L10, B18 and B18 + Gem mean values for the indicated times; One-way Anova. (**d**) Frequency of loops on B18 DNA incubated in extracts supplemented with buffer or treated with TPT at the start of reaction (TPT early) or after its completion at 300 minutes (TPT late) and collected one hour later. Experiments were repeated three times scoring the equivalent of about one mega base of total DNA. Error bars represent ± sd of the mean. n=3 experiments; p<0.001 when comparing B18 mean values for all treatments; One-way Anova. (**e**) Model illustrating arrangement and response to replication stress of centromeric chromatin, which is organized in loops of dsDNA formed in the presence of Condensins (*SMC2-4*) and active Topoisomerase I (Top I). Loops accumulate most likely behind replication forks. Individual centromeric repeats might form hairpins or other secondary structures on unwound ssDNA at replication forks, attracting MMR proteins, which might be required to resolve them (Panel a). This topological arrangement limits the formation of extensive ssDNA regions and *RPA* hyper-loading onto chromatin triggered by the uncoupling of helicase and polymerase induced by aphidicolin (APH) or other fork stalling events. Inhibition of *RPA* binding to chromatin prevents activation of *ATR*. ssDNA generated during fork uncoupling folds into several hairpins, leading to MMR proteins accumulation (Panel b). Interference with contromeric DNA topology by Toposimerase I inhibitor (TPT) restores *RPA* loading and *ATR* activity, which inhibits centromeric DNA replication (Panel c), suggesting that topology dependent suppression of *ATR* normally facilitates replication of hard-to-replicate repetitive DNA sequences present at the centromere.